Photoinduced dynamics in doped Mott insulators with polaronic conduction: $Ba_2Ti_{13}O_{22}$ and $Ba_xTi_8O_{16}$

N. Yamaguchi,[1] A. Furuhashi,[1] H. Nishihara,[1] R. Murata,[1] K. Takayama,[1] and T. Katsufuji[1,2,*]

[1]*Department of Physics, Waseda University, Tokyo 169-8555, Japan*

[2]*Kagami Memorial Research Institute for Materials Science and Technology, Waseda University, Tokyo 169-0051, Japan*

(Received 29 March 2016; revised manuscript received 31 May 2016; published 15 July 2016)

To clarify the dynamics of polarons in doped Mott insulators, we performed pump-probe reflectivity measurements for two barium titanates, $Ba_2Ti_{13}O_{22}$ and $Ba_xTi_8O_{16}$, with a noninteger average number of d electrons per Ti. We found that the photoinduced dynamics in $Ba_2Ti_{13}O_{22}$ with a three-dimensional electronic structure is characterized by a broadening of the polaron-excitation peak immediately after photoirradiation, whereas that in $Ba_xTi_8O_{16}$ with a one-dimensional electronic structure is characterized by a change in the intensities of the polaron-excitation peak and charge-gap-excitation peak with time. This indicates that a difference in dimensionality results in different photoinduced dynamics of polarons in doped Mott insulators.

DOI: 10.1103/PhysRevB.94.045119

I. INTRODUCTION

Non-Drude-like polaronic conduction is commonly observed in various doped transition-metal oxides [1]. When an undoped transition-metal oxide with an integer number of d electrons per site is insulating because of the on-site Coulomb repulsion between the d electrons, i.e., it is a so-called Mott insulator, a small amount of carrier doping should theoretically result in a metallic state. Experimentally, however, it usually becomes metallic only after the amount of doping exceeds a threshold, or it often remains insulating over the whole doping range [1]. One of the origins of such insulating behavior in a Mott insulator with a finite amount of doping is the coupling between the doped d electrons and the lattice distortion, which causes the formation of small polarons [2]. Occasionally, compounds with such polaronic conduction exhibit an electronic phase transition, for example, charge/orbital ordering, which can be understood as the ordering of small polarons [3–5].

Non-Drude-like polaronic conduction is experimentally characterized by a negative temperature derivative of electrical resistivity ($d\rho/dT$) and also by a peak structure in the optical conductivity spectrum [$\sigma(\omega)$] [6–11]. The latter is in contrast to the Drude spectrum of $\sigma(\omega)$ having a maximum at $\omega = 0$, which is characteristic of a metallic state. Associated with the charge/orbital ordering, such a peak structure shifts to higher energies ($\hbar\omega$) and a gap opens up in the $\sigma(\omega)$ spectrum.

The nature of such non-Drude-like conduction in doped transition-metal oxides is not yet well understood. Although we emphasized the role of electron-lattice coupling above, Anderson localization caused by disorder in the crystal and/or long-range Coulomb repulsion between the d electrons may also play an important role [12]. In the present study, we attempt to clarify the nature of such non-Drude-like conduction in transition-metal oxides by studying their optical properties and photoinduced dynamics. The photoinduced dynamics of doped Mott insulators have been studied only for a limited number of compounds [13–15]. We investigate two different compounds with different dimensionalities and study how such a difference causes different behaviors in the optical process of small polarons.

The compounds studied are $Ba_2Ti_{13}O_{22}$ [16] and hollandite $Ba_xTi_8O_{16}$ ($x = 1.13$) [17]. These two compounds have several characteristics in common. First, both compounds have Ti ions with an average valence between +4 and +3 and thus the number of d electrons per Ti (n) is between 0 and 1 ($n = 0.92$ for $Ba_2Ti_{13}O_{22}$ and $n \sim 0.2$ for $Ba_xTi_8O_{16}$). Second, both compounds exhibit an electronic phase transition at around ~200 K. Third, in the optical conductivity spectrum $\sigma(\omega)$, a clear peak structure (at $\hbar\omega \sim 0.5$ eV for $Ba_2Ti_{13}O_{22}$ and at $\hbar\omega \sim 0.9$ eV for $Ba_xTi_8O_{16}$) is observed, indicating electrical conduction by small polarons.

These compounds also have different characteristics. First, there is only slight anisotropy in both the electrical resistivity $\rho(T)$ and $\sigma(\omega)$ for $Ba_2Ti_{13}O_{22}$ [16], indicating the three-dimensional character of the conduction, whereas there is clear anisotropy in both quantities [$\rho_c(T) \ll \rho_a(T)$ and $\sigma_c(\omega) \gg \sigma_a(\omega)$] for $Ba_xTi_8O_{16}$ [17], indicating one-dimensional conduction along the Ti-O chains ($\| c$). This difference is correlated to the difference in the crystal structure, as schematically shown in the inset of Fig. 1(a) and Fig. 2(a). Namely, the TiO_6 octahedra are three-dimensionally connected in $Ba_2Ti_{13}O_{22}$, whereas they are aligned in the form of double chains along the c axis in $Ba_xTi_8O_{16}$.

Furthermore, below the transition temperature T_c, $\rho(T)$ monotonically increases and diverges at the lowest temperature (T) for $Ba_xTi_8O_{16}$ [17], indicating an insulating ground state. A modulation in the Ti-O chains was observed in the electron diffraction, indicating the ordering of d electrons (charge ordering) in $Ba_xTi_8O_{16}$ [17]. On the other hand, $\rho(T)$ slightly increases but decreases again with further decreasing T for $Ba_2Ti_{13}O_{22}$ [16], indicating a metallic character in the low-T phase. This suggests that the electrical conduction in $Ba_2Ti_{13}O_{22}$ is dominated by both small polarons and itinerant carriers, the latter of which yield a Drude component in the $\sigma(\omega)$ spectrum. This behavior is similar to that of a charge-density-wave (CDW) state, though the commensurate wave vector of the structural modulation and the linear T

*Author to whom correspondence should be addressed: katsuf@waseda.jp

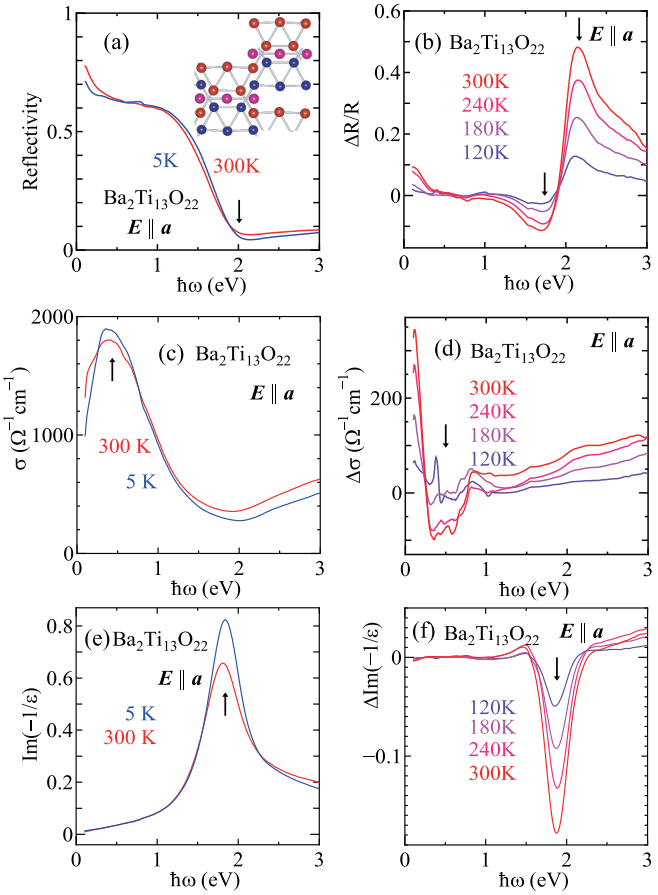

FIG. 1. (a) Steady-state optical reflectivity spectra, (b) the difference reflectivity spectra with T, (c) the optical conductivity spectra, (d) the difference conductivity spectra with T, (e) the loss function, and (f) the difference loss function with T for $Ba_2Ti_{13}O_{22}$ with $E \| a$. The inset of (a) shows the schematic picture of the crystal structure for $Ba_2Ti_{13}O_{22}$ (the Ti sites only).

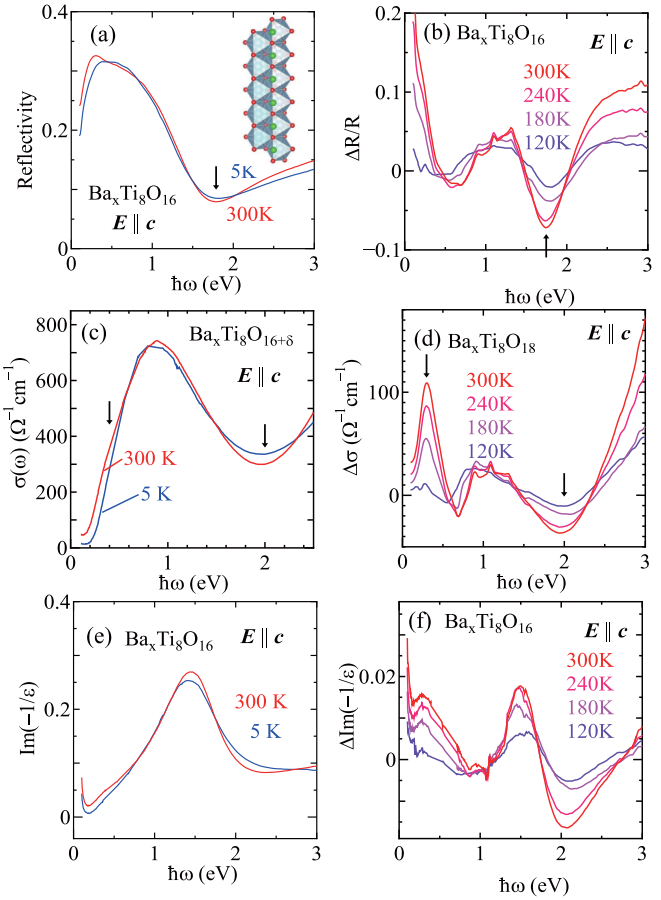

FIG. 2. (a) Steady-state optical reflectivity spectra, (b) difference reflectivity spectra with T, (c) optical conductivity spectra, (d) difference conductivity spectra with T, (e) loss function, and (f) difference loss function with T for $Ba_xTi_8O_{16}$ with $E \| c$. The inset of (a) shows the schematic picture of the crystal structure for $Ba_xTi_8O_{16}$ (TiO_6 octahedra only).

dependence of the magnetic susceptibility in the low T phase of $Ba_2Ti_{13}O_{22}$ are not compatible with such a simple CDW picture [16].

In the present study, we measured the photoinduced dynamics of these compounds by the pump-probe reflectivity technique, compared the results with the T dependence of their conventional (steady state) optical spectra, and analyzed the data, focusing on which changes in the parameters can reproduce the photoinduced changes in these two compounds.

II. EXPERIMENT

Single crystals of $Ba_2Ti_{13}O_{22}$ and $Ba_xTi_8O_{16}$ were grown by the floating-zone technique as described elsewhere [16,17]. For optical measurement, a cleaved surface of orthorhombic $Ba_2Ti_{13}O_{22}$ along the ab plane and a polished surface of tetragonal $Ba_xTi_8O_{16}$ along the ac plane were prepared. Time-resolved pump-probe measurement was performed as follows. The light pulse from a Ti:sapphire regenerative amplified laser (wavelength 795 nm, pulse width 130 fs, and repetition rate 1 kHz) was used as a pump pulse, and the light pulse from the same laser that was broadened in frequency ($\hbar\omega = 0.9$–2.5 eV) by self phase modulation of the light propagating in water was used as a probe pulse. The pump pulse was first applied to the sample surface and then the probe pulse was applied with a time delay t, which was controlled by changing the length of the route for the probe pulse. The reflected light of the probe pulse from the sample surface was monochromated, and the relative changes in reflectivity upon the irradiation of a pump pulse ($\Delta R/R$, photoinduced change in reflectivity) were obtained by a lock-in technique. The time resolution of the measurement was ∼250 fs. The sample was cooled to 10 K using a conduction-type He cryostat. The steady-state reflectivity spectra $R(\omega)$ were measured between 0.1 and 0.8 eV by an FTIR spectrometer and between 0.7 and 5 eV by a grating spectrometer. The optical conductivity $\sigma(\omega)$ and loss function $\mathrm{Im}[-1/\epsilon(\omega)]$ were obtained from the reflectivity spectra by the Kramers-Kronig (KK) transformation.

III. OPTICAL SPECTRA AND THEIR PHOTOINDUCED CHANGES FOR $Ba_2Ti_{13}O_{22}$ AND $Ba_xTi_8O_{16}$

Figures 1 and 2 show (a) the steady-state optical reflectivity spectra $R(\omega)$, (b) the difference reflectivity spectra with T, $\Delta R/R = [R(\omega)_T - R(\omega)_{5\,\mathrm{K}}]/R(\omega)_{5\,\mathrm{K}}$, (c) the optical

conductivity spectra $\sigma(\omega)$, (d) the difference conductivity spectra with T, $\Delta\sigma(\omega) = \sigma(\omega)_T - \sigma(\omega)_{5\,\mathrm{K}}$, (e) the loss function $\mathrm{Im}[-1/\epsilon(\omega)]$, and (f) the difference loss function with T, $\Delta\mathrm{Im}[-1/\epsilon(\omega)] = \mathrm{Im}[-1/\epsilon(\omega)]_T - \mathrm{Im}[-1/\epsilon(\omega)]_{5\,\mathrm{K}}$, for $Ba_2Ti_{13}O_{22}$ with $E\|a$ (Fig. 1) and for $Ba_xTi_8O_{16}$ with $E\|c$ (Fig. 2). For $Ba_2Ti_{13}O_{22}$, an edge exists at 2 eV in the $R(\omega)$ spectra [Fig. 1(a)], which sharpens with decreasing T. In the $\Delta R/R$ spectra [Fig. 1(b)], a dip at ~1.7 eV and a peak at ~2.1 eV evolve with increasing T, which are caused by the broadening of the edge in $R(\omega)$. For the $\sigma(\omega)$ spectra [Fig. 1(c)], a peak structure centered at ~0.4 eV, which corresponds to the polaron-excitation peak, exists both at 5 and 300 K, and the width of the peak decreases with decreasing T, generating a pseudogap in the $\sigma(\omega)$ spectrum below 0.2 eV [16]. The $\Delta\sigma(\omega)$ spectra [Fig. 1(d)] exhibit suppression at ~0.4 eV and an increase at ~0 eV.

For the $\mathrm{Im}[-1/\epsilon(\omega)]$ spectra [Fig. 1(e)], a peak exists at ~1.9 eV, which corresponds to the longitudinal mode of the polarons, whose transverse mode exists at ~0.4 eV in the $\sigma(\omega)$ spectra. The width of the peak in the $\mathrm{Im}[-1/\epsilon(\omega)]$ spectra decreases with decreasing T, and this causes the evolution of a dip at 1.9 eV in the $\Delta\mathrm{Im}[-1/\epsilon(\omega)]$ spectrum with increasing T [Fig. 1(f)]. Note that the change in the width of the peak in the $\mathrm{Im}[-1/\epsilon(\omega)]$ spectrum at 1.9 eV is correlated with the change in the width of the peak in the $\sigma(\omega)$ spectrum at 0.4 eV. Note also that $R(\omega)$ is dominated by both $\sigma(\omega)$ (transverse mode) and $\mathrm{Im}[-1/\epsilon(\omega)]$ (longitudinal mode) in general, but in the case of $Ba_2Ti_{13}O_{22}$, the change in $\Delta R/R$ at around 2 eV [Fig. 1(a)] is mostly dominated by the change in $\mathrm{Im}[-1/\epsilon(\omega)]$ [Fig. 1(f)], whereas $\sigma(\omega)$ hardly changes at this energy [Fig. 1(d)].

For $Ba_xTi_8O_{16}$, an edge exists at ~1.6 eV in the $R(\omega)$ spectra [Fig. 2(a)], similar to $Ba_2Ti_{13}O_{22}$. Unlike the case of $Ba_2Ti_{13}O_{22}$, however, the edge appears to sharpen with *increasing* T for $Ba_xTi_8O_{16}$. As a result, a dip evolves at ~1.7 eV in the $\Delta R/R$ spectrum with increasing T [Fig. 2(b)]. This seemingly unusual behavior is due to a structure in the $\sigma(\omega)$ spectrum at around 2 eV, which only appears below $T_c \sim 220$ K. As shown in Fig. 2(c), $\sigma(\omega)$ decreases below 0.6 eV but starts to increase at around 2 eV with decreasing T. This means that, associated with the electronic phase transition at $T_c \sim 220$ K, the spectral weight below 0.6 eV is suppressed and transferred to around 2 eV in $Ba_xTi_8O_{16}$ [17]. This can be more clearly seen in the $\Delta\sigma(\omega)$ spectrum in Fig. 2(d), where a peak at 0.4 eV and a dip at 2 eV evolve with increasing T. The difference between the peak position in the $\sigma(\omega)$ spectrum (~0.8 eV) and the dip position in the $\Delta\sigma(\omega)$ spectrum (~2.0 eV) suggests that at least two components are necessary to reproduce the change in the optical spectra with T for $Ba_xTi_8O_{16}$. The loss function and the difference loss function of the same compound are respectively shown in Figs. 2(e) and 2(f). In $Ba_xTi_8O_{16}$, both the change in $\sigma(\omega)$ [Fig. 2(d)] and that in $\mathrm{Im}[-1/\epsilon(\omega)]$ [Fig. 2(f)] contribute to the change in $R(\omega)$ [Fig. 2(b)].

We measured the photoinduced changes in reflectivity for these compounds, and typical photoinduced $\Delta R/R$ spectra with t (delay time) of 0.3 and 10 ps at $T = 10$ K are shown in Fig. 3 for (a) $Ba_2Ti_{13}O_{22}$ and (b) $Ba_xTi_8O_{16}$ [18]. The two spectra at $t = 0.3$ and 10 ps for $Ba_2Ti_{13}O_{22}$ [Fig. 3(a)] are almost the same and exhibit a dip at ~1.8 eV and a peak at

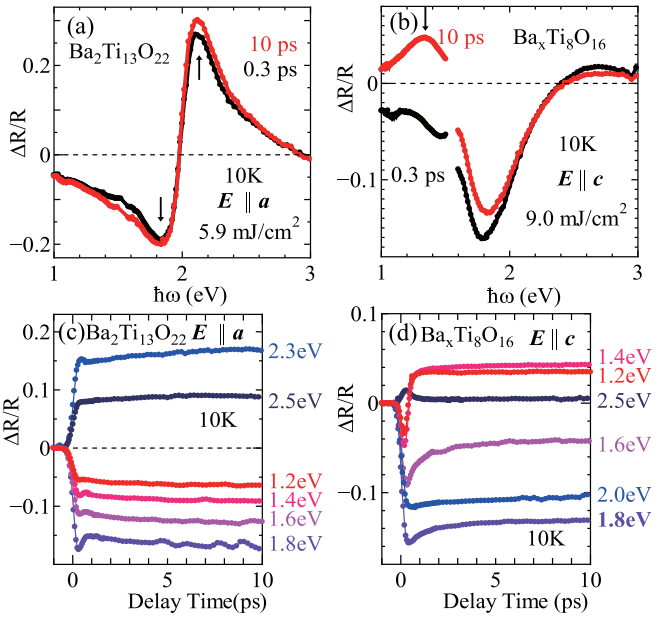

FIG. 3. Photoinduced changes in reflectivity as a function of $\hbar\omega$ for (a) $Ba_2Ti_{13}O_{22}$ and (b) $Ba_xTi_8O_{16}$ and as a function of the delay time for (c) $Ba_2Ti_{13}O_{22}$ and (d) $Ba_xTi_8O_{16}$.

~2.1 eV, where the photoinduced $|\Delta R/R|$ exceeds 20%. As shown in Fig. 4(a), this photoinduced change in reflectivity is similar to the difference reflectivity spectrum at $T = 240$ K. This means that the $R(\omega)$ spectrum at 10 K is changed into that at 240 K within 0.3 ps after the irradiation of a pump pulse, then remains unchanged for more than 10 ps. Figure 3(c) shows the photoinduced $\Delta R/R$ as a function of the delay time t at various values of $\hbar\omega$ for the probe pulse. $\Delta R/R$ changes immediately after the irradiation of a pump pulse at $t = 0$ ps and then remains unchanged for over 10 ps for all values of $\hbar\omega$ in the case of $Ba_2Ti_{13}O_{22}$.

On the other hand, the photoinduced $\Delta R/R$ spectrum for $Ba_xTi_8O_{16}$ [Fig. 3(b)] at $t = 0.3$ ps is different from that at 10 ps; the sign of $\Delta R/R$ at around 1.4 eV is negative at 0.3 ps, whereas it becomes positive at 10 ps. As shown in Fig. 3(d), $\Delta R/R$ with $\hbar\omega = 1.2$ and 1.4 eV becomes negative immediately after the irradiation of a pump pulse at $t = 0$ ps but becomes positive within 1 ps. This means that there are two components that vary in different time scales after the

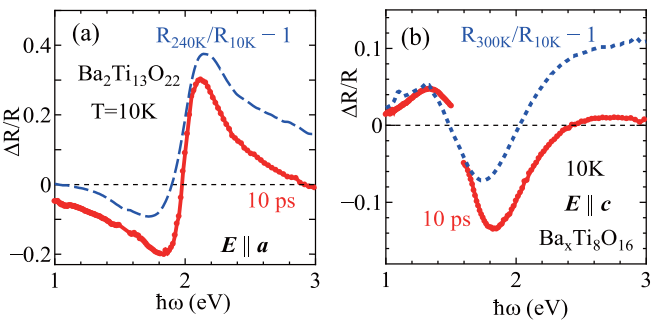

FIG. 4. Comparison between the photoinduced changes in reflectivity (solid lines) and the difference reflectivity spectra with T (dashed lines) for (a) $Ba_2Ti_{13}O_{22}$ and (b) $Ba_xTi_8O_{16}$.

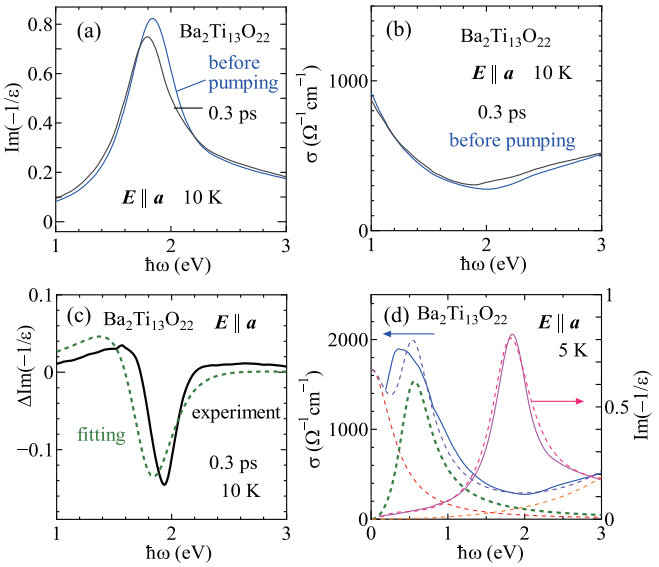

FIG. 5. (a) Loss function and (b) optical conductivity spectra before photoirradiation (pumping) and 0.3 ps after photoirradiation at 10 K, (c) experimental (solid line) and calculated (dashed line) results of the photoinduced change in the loss function at 10 K, and (d) experimental (solid lines) and calculated (dashed lines) results of the (steady-state) optical conductivity $\sigma(\omega)$ and loss function $\mathrm{Im}[-1/\epsilon(\omega)]$ at 5 K for $Ba_2Ti_{13}O_{22}$.

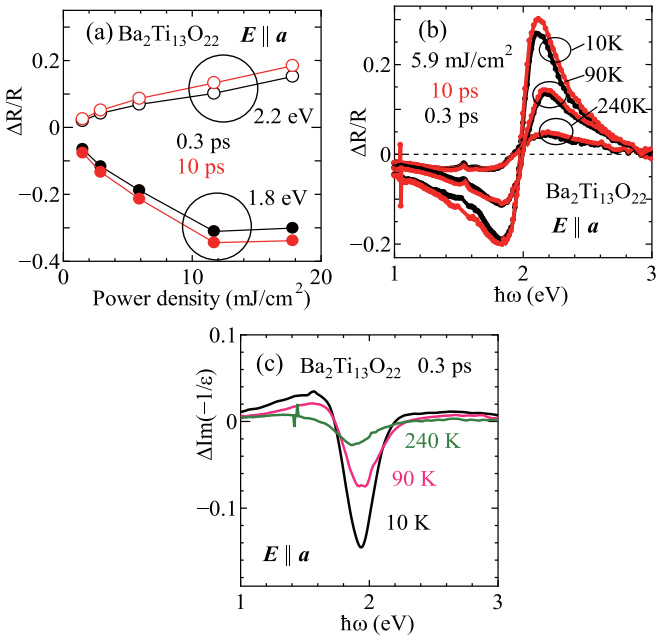

FIG. 6. (a) Dependence of the photoinduced change in reflectivity on the power density of the pump pulse with $\hbar\omega = 1.8$ and 2.2 eV for the probe pulse at 10 K, (b) photoinduced change in the reflectivity spectra at various temperatures, and (c) photoinduced change in the loss function at various temperatures for $Ba_2Ti_{13}O_{22}$.

application of a pump pulse. Figure 4(b) shows a comparison between the photoinduced change in reflectivity at 10 ps and the difference reflectivity spectra at $T = 300$ K. The similarity between the two spectra indicates that at least 10 ps after the photoirradiation, the reflectivity spectrum becomes that at 300 K for $Ba_xTi_8O_{16}$.

IV. ANALYSIS OF THE PHOTOINDUCED CHANGE IN THE OPTICAL SPECTRUM FOR $Ba_2Ti_{13}O_{22}$

In this section, we analyze the photoinduced $\Delta R/R$ spectra for $Ba_2Ti_{13}O_{22}$. Figures 5(a) and 5(b) show the loss function $\mathrm{Im}[-1/\epsilon(\omega)]$ and optical conductivity $\sigma(\omega)$, respectively, before the application of the pump pulse and 0.3 ps after its application, which were obtained by the KK transformation of the $R(\omega)$ and photoinduced $R(\omega)$ spectra. The peak in the $\mathrm{Im}[-1/\epsilon(\omega)]$ spectrum at 1.8 eV is suppressed and broadened at $t = 0.3$ ps, whereas only a slight increase is observed in the $\sigma(\omega)$ spectrum at 0.3 ps. This is similar to the change in the optical spectra with T shown in Figs. 1(c) and 1(e), and suggests that the photoinduced $\Delta R/R$ can be reproduced by increasing the width of the polaron-excitation spectrum.

We first fitted the $\sigma(\omega)$ spectrum of $Ba_2Ti_{13}O_{22}$ at 5 K using the sum of one Drude term and two Lorentz terms,

$$\epsilon(\omega) = \epsilon_\infty - \frac{\omega_p^2}{\omega^2 + i\omega\gamma_p} + \sum_{i=1}^{2} \frac{S_i\omega_i^2}{\omega_i^2 - \omega^2 - i\omega\gamma_i}, \quad (1)$$

$$\sigma(\omega) = \mathrm{Im}\{\omega\epsilon(\omega)\}. \quad (2)$$

The optical conductivity $\sigma(\omega)$ and loss function $\mathrm{Im}[-1/\epsilon(\omega)]$ experimentally obtained (solid lines) and calculated by Eq. (1) (dashed lines) are shown in Fig. 5(d). The Lorentz term at lower $\hbar\omega_i$ ($\hbar\omega_1 = 0.56$ eV, $\hbar\gamma_1 = 0.52$ eV, and $S_1 = 18.5$) corresponds to the excitation of small polarons.

To reproduce the photoinduced change in the optical spectra, we found that it is sufficient to change only the width of the small-polaron excitation, γ_1. Figure 5(c) shows the experimental result (solid line) and calculated result (dashed line) of $\Delta\mathrm{Im}[-1/\epsilon(\omega)]$ when $\hbar\gamma_1$ changes from 0.52 eV to 0.76 eV. The reasonably good agreement between the experimental and calculated results means that upon the application of a pump pulse, the width of the polaron-excitation peak is increased by 0.24 eV within 0.3 ps.

Figure 6(a) shows the photoinduced $\Delta R/R$ at $\hbar\omega = 1.8$ and 2.2 eV for the probe pulse, which correspond to the dip and peak positions in the photoinduced $\Delta R/R$ spectrum shown in Fig. 3(a), as a function of the power density of the pump pulse at 10 K. The absolute value of $\Delta R/R$ increases almost linearly with the power density at 2.2 eV but shows saturation behavior at 1.8 eV. Figure 6(b) shows the photoinduced $\Delta R/R$ spectra taken at various temperatures, and Fig. 6(c) shows the photoinduced $\Delta\mathrm{Im}[-1/\epsilon(\omega)]$ at $t = 0.3$ ps obtained from the KK transformation of the $\Delta R/R$ spectra. As can be seen, the absolute value of the photoinduced change in the optical spectrum decreases with increasing T, but the overall features of the spectrum do not change even above $T_c = 200$ K. These results suggest that irrespective of T and the power density of the pump pulse, the photoinduced change in the optical spectrum is dominated by the increase in the width of the polaron-excitation peak for $Ba_2Ti_{13}O_{22}$.

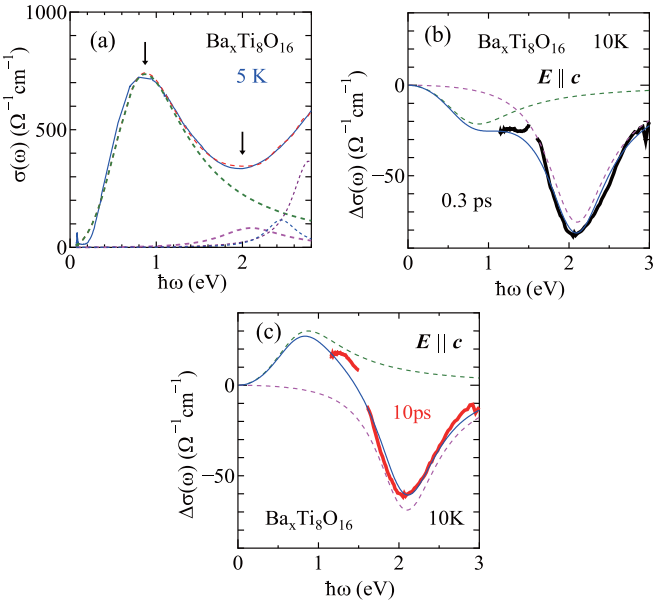

FIG. 7. (a) Fitting of the (steady state) optical conductivity spectrum at 5 K, and (b),(c) experimental (thick solid lines) and calculated (thin solid lines) results obtained with each Lorentz term (dashed lines) for the photoinduced change in the optical conductivity at (b) $t = 0.3$ ps and (c) $t = 10$ ps for $Ba_xTi_8O_{16}$.

V. ANALYSIS OF THE PHOTOINDUCED CHANGE IN THE OPTICAL SPECTRUM FOR $Ba_xTi_8O_{16}$

In this section, we analyze the photoinduced change in the optical spectrum for $Ba_xTi_8O_{16}$. Figure 7(a) shows the result of fitting the optical conductivity spectrum $\sigma(\omega)$ for $Ba_xTi_8O_{16}$ at 5 K using four Lorentz terms,

$$\epsilon(\omega) = \epsilon_\infty + \sum_{i=1}^{4} \frac{S_i \omega_i^2}{\omega_i^2 - \omega^2 - i\omega\gamma_i}, \tag{3}$$

$$\sigma(\omega) = \mathrm{Im}\{\omega\epsilon(\omega)\}. \tag{4}$$

The Lorentz term with the lowest $\hbar\omega_i$ ($\hbar\omega_1 = 0.87$ eV, $\hbar\gamma_1 = 1.1$ eV, and $S_1 = 7.76$) corresponds to the excitation of small polarons and that with the second lowest $\hbar\omega_i$ ($\hbar\omega_2 = 2.1$ eV, $\hbar\gamma_2 = 0.9$ eV, and $S_2 = 0.12$) corresponds to the excitation across the charge gap associated with the electronic phase transition at $T_c = 200$ K. Note that the dip at 2 eV observed in the difference optical conductivity spectrum with T shown in Fig. 2(d) is caused by the suppression of this peak at 2.1 eV above T_c.

On the basis of this fitting, we found that the photoinduced change in the optical spectra can be reproduced by simply changing the oscillator strengths of the polaron-excitation peak at 0.86 eV (S_1) and the charge-gap-excitation peak at 2.1 eV (S_2). Figures 7(b) and 7(c) show the experimental result of the photoinduced change in the optical conductivity [$\Delta\sigma(\omega)$] obtained by the KK transformation and the calculated change in the optical conductivity when S_1 decreases from 7.76 to 7.53 and S_2 decreases from 0.12 to 0.01 for $t = 0.3$ ps [Fig. 7(b)], and when S_1 increases from 7.76 to 8.08 and S_2 decreases from 0.12 to 0.02 for $t = 10$ ps [Fig. 7(c)]. This result means that upon the application of a pump pulse, both

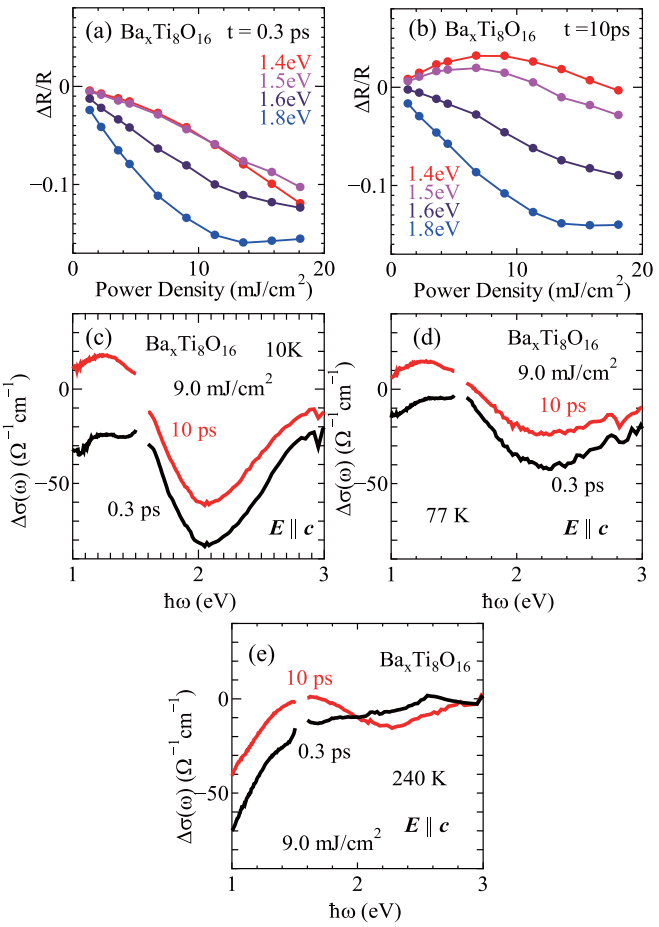

FIG. 8. (a),(b) Dependence of the photoinduced change in reflectivity on the power density of the pump pulse at (a) $t = 0.3$ ps and (b) $t = 10$ ps with various values of $\hbar\omega$ for the probe pulse, and (c),(d),(e) photoinduced change in the optical conductivity at (c) 10 K, (d) 77 K, and (e) 240 K for $Ba_xTi_8O_{16}$.

the polaron excitation peak at 0.87 eV and the charge-gap-excitation peak at 2.1 eV are suppressed within 0.3 ps, and then the polaron-excitation peak increases in intensity but the charge-gap-excitation peak remains suppressed at 10 ps.

Note that the sum rule should hold for the photoinduced $\Delta\sigma(\omega)$ spectrum in general and, in this regard, the experimentally obtained photoinduced $\Delta\sigma(\omega)$ spectrum at 0.3 ps, which is always negative between $\hbar\omega = 1$ and 3 eV as shown in Fig. 7(c), should be positive outside this range. It is most likely that a Drude component appears below 1 eV and compensates the photoinduced suppression of the polaron-excitation and charge-gap-excitation peaks. Note that the appearance of a Drude component in the photoinduced optical spectrum has been reported for various one-dimensional Mott insulators without chemical doping [19,20].

Figures 8(a) and 8(b) show the photoinduced $\Delta R/R$ at various values of $\hbar\omega$ for the probe pulse as a function of the power density of the pump pulse at $t = 0.3$ and 10 ps, respectively. The decrease in $\Delta R/R$ at 1.8 eV, which corresponds to the photoinduced suppression of the charge-gap-excitation peak at 2.1 eV in the $\sigma(\omega)$ spectrum, is saturated above 10 mJ/cm^2 for both $t = 0.3$ and 10 ps.

This means that the charge-gap-excitation peak that appears in association with the electronic phase transition at $T_c = 220$ K is fully suppressed if a sufficiently strong pump pulse is applied to the compound. Figures 8(c), 8(d), and 8(e) show the photoinduced $\Delta R/R$ spectra at 10, 77, and 240 K ($>T_c$), respectively. The dip at 2 eV decreases and almost disappears at 240 K. This corresponds to the disappearance of the charge-gap-excitation-peak above T_c in $Ba_xTi_8O_{16}$. Such complicated behaviors of the power-density dependence and T dependence in $Ba_xTi_8O_{16}$ are in clear contrast to the simple behaviors of the same quantities in $Ba_2Ti_{13}O_{22}$ shown in Fig. 6.

VI. DISCUSSION

Schematic diagrams of the photoinduced dynamics in $Ba_2Ti_{13}O_{22}$ and $Ba_xTi_8O_{16}$ are shown in Fig. 9. For both compounds, the photoinduced change in the spectrum at $t = 10$ ps [Figs. 9(b) and 9(d)] is similar to the difference spectra at higher T. This means that the photoinduced change at $t = 10$ ps is mainly dominated by the thermal heating induced by the irradiation of a pump pulse. For $Ba_2Ti_{13}O_{22}$, the photoinduced change in the spectrum at $t = 0.3$ ps [Fig. 9(a)] is also similar to the thermally induced change, and all the changes are dominated by the broadening of the polaron-excitation peak. In terms of the photoinduced change in reflectivity for $Ba_2Ti_{13}O_{22}$, which we measured between 1 and 3 eV in the present study, the change in the longitudinal mode [loss function $\mathrm{Im}(-1/\epsilon)$] shown by dashed lines in Figs. 9(a) and 9(b) is dominant compared with the change in the optical conductivity in the transverse mode.

For $Ba_xTi_8O_{16}$, the photoinduced change in the spectrum at $t = 0.3$ ps [Fig. 9(c)] is qualitatively different from that at $t = 10$ ps [Fig. 9(d)]. At 10 ps after the photoirradiation [Fig. 9(d)], the charge-gap-excitation peak is suppressed and the spectral weight is transferred to the polaron-excitation peak at a lower $\hbar\omega$. This can be regarded as the thermally induced change with the irradiation of a pump pulse. However, at 0.3 ps after the photoirradiation [Fig. 9(c)], both the charge-gap-excitation peak and the polaron-excitation peak are suppressed, and it is likely that the spectral weight is transferred to the Drude peak at $\hbar\omega \sim 0$ eV. This difference between the photoinduced change at 0.3 ps and the thermally induced change causes the complicated time evolution [Fig. 4(d)], the complicated power-density and T dependences (Fig. 8) of the photoinduced $\Delta R/R$ for $Ba_xTi_8O_{16}$.

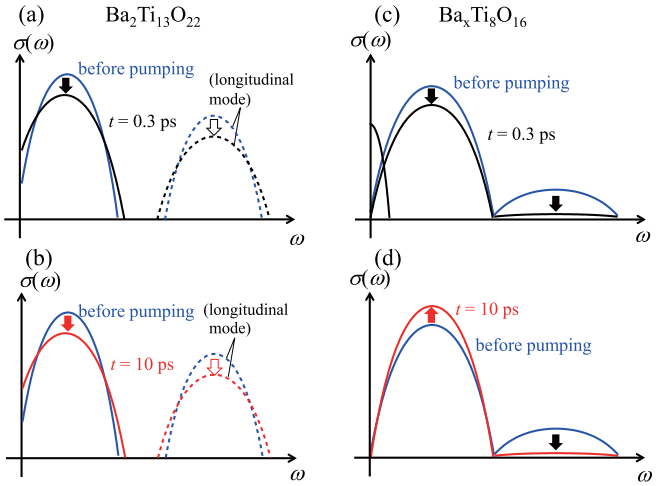

FIG. 9. Schematic diagrams of the photoinduced changes in the optical conductivity for (a),(b) $Ba_2Ti_{13}O_{22}$ and (c),(d) $Ba_xTi_8O_{16}$ at (a),(c) $t = 0.3$ ps and (b),(d) $t = 10$ ps.

The different behaviors of the photoinduced dynamics between $Ba_2Ti_{13}O_{22}$ and $Ba_xTi_8O_{16}$ are caused by the different changes in the $\sigma(\omega)$ spectra with the phase transition. For $Ba_2Ti_{13}O_{22}$, the polaron-excitation peak itself is narrowed and a pseudogap opens below T_c. For $Ba_xTi_8O_{16}$, the spectral weight of the polaron-excitation peak is transferred to a charge-gap-excitation peak at a higher $\hbar\omega$ ($\sim$2 eV) below T_c. It is likely that this difference in the T dependence of the $\sigma(\omega)$ spectra is related to the difference in dimensionality. Namely, in hollandite $Ba_xTi_8O_{16}$ having quasi-one-dimensional Ti-O chains, the polarons on the one-dimensional chains are aligned periodically and generate a charge gap whose energy scale ($\sim$2 eV) is higher than the binding energy of the polarons ($\sim$0.3 eV) [17]. On the other hand, the energy scale of the pseudogap in $Ba_2Ti_{13}O_{22}$ below T_c is lower than the binding energy of the polarons ($\sim$1 eV) [16]. Thus the difference in dimensionality between the two compounds leads to the difference in the change of the $\sigma(\omega)$ spectra across T_c, resulting in the different time evolution of the photoinduced optical spectra.

VII. SUMMARY

We studied the photoinduced dynamics of $Ba_2Ti_{13}O_{22}$ and $Ba_xTi_8O_{16}$, both of which exhibit the polaronic conduction of Ti d electrons and an electronic phase transition at $\sim$200 K. It was found that the photoinduced dynamics of $Ba_2Ti_{13}O_{22}$ with a three-dimensional electronic structure can be explained by the broadening of a polaron-excitation peak immediately after photoirradiation ($<$0.3 ps). On the other hand, for $Ba_xTi_8O_{16}$ with a one-dimensional electronic structure, the intensities of both the polaron-excitation peak and the charge-gap-excitation peak, the latter of which appears only below the transition temperature, decrease immediately after the photoirradiation. In contrast, the polaron-excitation peak acquires more intensity than that before the phoroirradiation within several picoseconds while the charge-gap-excitation peak remains suppressed. Such different photoinduced dynamics are caused by the different changes in the optical spectra with the phase transition in the two compounds. Namely, the polaron-excitation peak is narrowed and a pseudogap opens below T_c for $Ba_2Ti_{13}O_{22}$, whereas the intensity of the polaron-excitation peak decreases and the spectral weight is transferred to the charge-gap-excitation peak at higher energies for $Ba_xTi_8O_{16}$. This difference probably arises from the difference in dimensionality between these two compounds.

ACKNOWLEDGMENT

This work was partly supported by JSPS KAKENHI Grant No. 25287090.

[1] M. Imada, A. Fujimori, and Y. Tokura, Rev. Mod. Phys. **70**, 1039 (1998).
[2] I. G. Austin and N. F. Mott, Adv. Phys. **18**, 41 (1969).
[3] C. H. Chen, S.-W. Cheong, and A. S. Cooper, Phys. Rev. Lett. **71**, 2461 (1993).
[4] A. J. Millis, Nature (London) **392**, 147 (1998).
[5] P. Abbamonte, G. Blumberg, A. Rusydi, A. Gozar, P. G. Evans, T. Siegrist, L. Venema, H. Eisaki, E. D. Isaacs, and G. A. Sawatzky, Nature (London) **431**, 1078 (2004).
[6] H. G. Reik and D. Heese, J. Phys. Chem. Solids **28**, 581 (1967).
[7] L. Degiorgi, P. Wachter, and D. Ihle, Phys. Rev. B **35**, 9259 (1987).
[8] T. Katsufuji, T. Tanabe, T. Ishikawa, Y. Fukuda, T. Arima, and Y. Tokura, Phys. Rev. B **54**, R14230 (1996).
[9] T. Osafune, N. Motoyama, H. Eisaki, and S. Uchida, Phys. Rev. Lett. **78**, 1980 (1997).
[10] H. L. Liu, S. L. Cooper, and S.-W. Cheong, Phys. Rev. Lett. **81**, 4684 (1998).
[11] C. Presura, M. Popinciuc, P. H. M. van Loosdrecht, D. van der Marel, M. Mostovoy, T. Yamauchi, and Y. Ueda, Phys. Rev. Lett. **90**, 026402 (2003).
[12] N. Mott, *Metal-Insulator Transitions* (Taylor & Francis, London, 1990).
[13] M. Matsubara, Y. Okimoto, T. Ogasawara, Y. Tomioka, H. Okamoto, and Y. Tokura, Phys. Rev. Lett. **99**, 207401 (2007).
[14] Y. Okimoto, X. Peng, M. Tamura, T. Morita, K. Onda, T. Ishikawa, S. Koshihara, N. Todoroki, T. Kyomen, and M. Itoh, Phys. Rev. Lett. **103**, 027402 (2009).
[15] R. Fukaya, Y. Okimoto, M. Kunitomo, T. Ishikawa, K. Onda, S. Koshihara, A. Isayama, and T. Sasagawa, J. Phys. Soc. Jpn. **82**, 083707 (2013).
[16] K. Takayama, T. Koyama, S. Mori, K. Kato, M. Takata, J. Fujioka, Y. Tokura, J. Miyazaki, and T. Katsufuji, Phys. Rev. Lett. **110**, 196405 (2013).
[17] R. Murata, T. Sato, T. Okuda, Y. Horibe, H. Tsukasaki, S. Mori, N.Yamaguchi, K. Sugimoto, S. Kawaguchi, M. Takata *et al.*, Phys. Rev. B **92**, 220408(R) (2015).
[18] The intensities of the pump pulse are the same as those shown in Fig. 3 for all other measurements unless specified.
[19] S. Iwai and H. Okamoto, J. Phys. Soc. Jpn. **75**, 011007 (2006).
[20] H. Matsuzaki, H. Nishioka, H. Uemura, A. Sawa, S. Sota, T. Tohyama, and H. Okamoto, Phys. Rev. B **91**, 081114(R) (2015).